Geochemical Journal, Vol. 50, pp. 315 to 325, 2016 doi:10.2343/geochemj.2.0418

Major elements and noble gases of the Jinju (H5) meteorite, an observed fall on March 9, 2014, in South Korea

KEISUKE NAGAO,[1,2]* MAKIKO K. HABA,[2,3] JONG IK LEE,[1] TAEHOON KIM,[1] MI JUNG LEE,[1] CHANGKUN PARK,[1] YONG JOO JWA[4] and BYEON-GAK CHOI[5]

[1]Korea Polar Research Institute, 26 Songdomirae-ro, Yeonsu-gu, Incheon 21990, South Korea
[2]Geochemical Research Center, Graduate School of Science, The University of Tokyo, Bunkyo-ku, Tokyo 113-0033, Japan
[3]Institute of Geochemistry and Petrology, ETH Zürich, 8092 Zürich, Switzerland
[4]Department of Geology, Gyeongsang National University, 501, Jinju-daero, Jinju 660-701, South Korea
[5]Department of Earth Science Education, Seoul National University, Silliing-dong, Gwanak-gu, Seoul 08826, South Korea

(*Received November 17, 2015; Accepted February 15, 2016*)

The Jinju (H5) meteorite fell as four fragments in the Jinju area, Gyeonsangnam-do, South Korea, on March 9, 2014. The major element concentrations and noble gas isotopic compositions were determined for Jinju-1 and Jinju-2, stones of the first and second discoveries, respectively, by using X-ray fluorescence (XRF) analysis and noble gas mass spectrometry combined with total melting and stepwise heating noble gas extraction. The major element composition agrees well with that of equilibrated H chondrites. Very low contamination from terrestrial atmospheric noble gases was detected, which may be attributed to the rapid recovery of the stones within two days after the fall of the Jinju meteorite. A short cosmic ray exposure age of 2.4 My was obtained. The (U,Th)-He, and K-Ar ages are concordant at *ca*. 4.0 Gy, which suggests that no severe heating event occurred to cause a loss of He after the resetting at 4.0 Gy. Overabundances of trapped Ar and Kr, which were released at 800°C, were found in addition to "normal" Q gas of Ar, Kr and Xe at ≥1400°C. The low-temperature component could be explained by Ar and Kr supplied by an adjacent impact region that were trapped when the minerals of the Jinju meteorite were formed during cooling. The heavy shock event that occurred at 4.0 Gy might have produced the observed numerous vugs and vapor growth crystals in this meteorite (Choi *et al*., 2015) and could have supplied the Ar and Kr to thermally weak minerals.

Keywords: Jinju (H5) chondrite, observed fall in Korea, noble gas, elemental composition, cosmic ray exposure and gas retention ages

INTRODUCTION

On March 9, 2014, at 20:04 KST, a sonic boom was heard, and a fireball traveling more than 100 km was observed that disappeared above the Gyeonsangnam-do, Jinju area in the southernmost part of South Korea. A stone with mass of 9 kg, referred to as Jinju-1, was found in Daegok-myeon, Jinju, by a farmer on the ground in his plastic greenhouse on the following morning (March 10). A second stone known as Jinju-2, at 4.1 kg, was discovered in Micheon-myeon, Jinju, on March 11, one day after the discovery of Jinju-1. Two additional stones weighing 0.4 kg and 20.5 kg, respectively, were recovered within 5 km from the location of the Jinju-1 a few days after the fireball observation in Jinju area. No rain fell between the observation of the fireball and the recovery of four stones, which had a combined weight of 34 kg. Each of the stones was almost completely covered with fusion crust, and their petrological characteristics are identical. They were taken to either Seoul National University or Korea Polar Research Institute (KOPRI) for scientific investigation. The meteorite was classified as an H5 ordinary chondrite on the basis of petrological, chemical, and oxygen isotope analysis (Choi *et al*., 2015). The Jinju meteorite is characterized by high porosity, at 19.5 vol.%, and low bulk density of 2.93 g/cm^3 owing to numerous vugs that might have been produced by a heavy shock event at S3 or higher (Choi *et al*., 2015). These vugs appear between chondrules as well as in inside some chondrules, with euhedral or subhedral crystals extending from the wall of the pores. These characteristics are similar to those previously reported in chondrites having vugs (Choi *et al*., 2015) such as Farmington (L5), Orvinio (H6), and Tadjera (L5) in Olsen (1981) and references therein, Yanzhuang (H6) in Xie and Chen (1997), Baszkówka (L5) and Mount Tazerzait (L5) in Wlotzka and Otto (2001). A possible scenario for the production of the crystals is that sufficient impact shock energy was transferred to increase the temperature high enough for vaporization of the fine-grained minerals, which was fol-

*Corresponding author (e-mail: nagao@kopri.re.kr)

lowed by recrystallization from the vapor (Choi *et al*., 2015).

We measured the noble gases of Jinju-1 and Jinju-2 to investigate the cosmic ray exposure, (U,Th)-He, and K-Ar ages, the conditions of cosmic ray irradiation in space, and the primordial noble gas concentrations to examine the history before and after ejection from the parent body of the Jinju meteorite. The noble gas data for the same stones from the Jinju meteorite have been reported at the 78th Annual Meeting of the Meteoritical Society (Nagao *et al*., 2015). In the present study, we discuss in detail the characteristics of the noble gases of the Jinju meteorite.

Experimental Methods

X-ray fluorescence analysis of chemical composition

The concentrations of 10 elements including Si, Al, Fe, Na, Mg, P, K, Ca, Ti, and Mn were determined for both Jinju-1 and Jinju-2 through X-ray fluorescence (XRF) at KOPRI. The technique applied for the Jinju meteorite was principally the same as that described in Fitton *et al*. (1998) and Fitton and Godard (2004). The analysis was conducted by using three glass beads prepared for each stone. To create the glass beads, powdered samples were ignited in a muffle furnace for 20 h at 1000°C. A 0.600 g aliquot of the powder was then mixed with 6.000 g of $Li_2B_4O_7$ and 0.050 g of LiBr in a Pt crucible. Fusion was conducted with an automated bead sampler (K2 Prime, Katanax Inc., Quebec, Canada) by 300 s pre-fusion at ~1050°C, followed by 60 s fusion at ~1080°C with agitation. Analysis of the elements was conducted by measuring the Kα lines through XRF with an Rh anode X-ray tube (Axios, PANalytical B.V., The Netherlands). The respective tube currents and voltages were 50–100 mA and 30–60 kV for Fe, Mn, Ti, and Ca, and 125 mA and 24 kV for the other elements.

Noble gas mass spectrometry

We measured the noble gases for Jinju-1 and Jinju-2, which were recovered within two days after the observed fall, by using fragments free of fusion crust taken from the interiors of the stones. Noble gases were measured for two fragments with masses of 22.1 mg and 130.5 mg taken from Jinju-1 and one fragment of 49.9 mg from Jinju-2. No treatments such as crushing and washing in water were applied to the samples before loading in the vacuum line. We used a modified-VG5400/MS-3 mass spectrometer at the Geochemical Research Center, The University of Tokyo, following the procedure described in Nagao *et al*. (2008). The samples were loaded in the side arms of a sample holder composed of borosilicate glass attached to a newly constructed extraction furnace designed for small samples. The furnace is connected to a noble gas purification line constructed in 2010 for noble gas analysis of the Hayabusa samples returned from asteroid Itokawa (Nagao *et al*., 2011). The samples were pre-heated in an ultrahigh vacuum at 150°C for about one day to remove atmospheric contamination. For noble gas extraction, the sample was dropped into a Mo crucible placed in a Ta tube, which can be heated from the outside by radiation emitted from an electric resistance W-heater. The heating temperature is controlled by a computer program controlling electric current to the W-heater while monitoring the temperature through a W-Re thermocouple set outside the Ta tube. Noble gases were extracted from the 22.1 mg Jinju-1 sample by total melting at 1800°C, and from the 130.5 mg Jinju-1 and 49.9 mg Jinju-2 samples by stepwise heating at the temperatures of 300°C, 800°C, 1100°C, 1400°C, and 1800°C. During the stepwise heating experiment, the furnace was cooled down to room temperature after each heating, and the evolved noble gases were measured prior to the next temperature step.

The gases evolved from the samples at each temperature step were purified by using two getter pumps (NP10, SAES Getters S.p.A. in Italy). Among the purified noble gases, Ne, Ar, Kr, and Xe were adsorbed onto a cryogenically cooled sintered stainless-steel trap (hereafter cryotrap) at 20 K for 5–10 min, after which time the metal valve of the cryotrap was closed. He, which remained as a gas phase, was first introduced into the mass spectrometer for isotope analysis. Afterward, Ne, Ar, Kr, and Xe were successively desorbed from the cryotrap at the temperatures of 50 K, 110 K, 150 K, and 230 K, respectively, and were measured by the mass spectrometer. Unseparated gas in each separation process was monitored by measuring the intensity of the representative isotope spectrum in each noble gas fraction. For example, because Kr partly appears in both Ar and Xe fractions, the ^{84}Kr intensities in Ar, Kr, and Xe fractions were measured and summed to calculate the absolute abundance of ^{84}Kr. He, Ne, and Ar were measured with a Daly-multiplier ion collector, and Kr and Xe were measured by using an ion counting system.

The sensitivities and mass discrimination correction factors were calculated by measuring a known amount of atmosphere stored in a metal container. The mass discrimination for ^{3}He/^{4}He was determined by using an ^{3}He-^{4}He mixture with ^{3}He/^{4}He = 1.71×10^{-4} stored in a different metal container. Uncertainty in the ^{3}He/^{4}He ratio of the mixture was estimated to be ≈1% (Nagao *et al*., 2010). Blank corrections were applied to the noble gas data.

Results

Chemical compositions

The concentrations of 10 elements of Jinju-1 and Jinju-2 are presented in Table 1. Although the elemental con-

Table 1. Chemical compositions (wt.%) of Jinju-1 and Jinju-2 measured with XRF

Sample	Si	Al	Fe	Na	Mg	P	K	Ca	Ti	Mn
Jinju-1	16.55	1.02	26.56	0.56	14.54	0.11	0.07	1.09	0.06	0.23
Jinju-1	16.66	1.04	26.60	0.58	14.47	0.12	0.08	1.18	0.07	0.23
Jinju-1	16.50	1.04	26.67	0.56	14.30	0.11	0.08	1.23	0.07	0.23
average	16.57	1.03	26.61	0.57	14.43	0.11	0.08	1.17	0.06	0.23
Jinju-2	16.55	1.00	27.28	0.54	14.64	0.12	0.07	1.08	0.07	0.23
Jinju-2	16.73	1.03	27.26	0.54	14.57	0.12	0.07	1.14	0.07	0.23
Jinju-2	16.55	1.04	27.31	0.55	14.32	0.12	0.08	1.21	0.07	0.24
average	16.61	1.02	27.28	0.54	14.51	0.12	0.08	1.14	0.07	0.23

XRF data were given by oxides, total of which were 103% in average.

centrations obtained by the XRF analysis were given in oxides, the recalculated element concentrations are presented in Table 1 for convenience in calculating the production rates of the cosmogenic isotopes ^{3}He, ^{21}Ne, and ^{38}Ar, as discussed below. Identical elemental compositions between Jinju-1 and Jinju-2 support that the two stones are derived from a single meteoroid that exploded into several fragments during passage through Earth's atmosphere. The concentrations of the 10 elements in Jinju, L, LL, and R chondrites are plotted in Fig. 1 against their concentrations in H chondrites (Lodders and Fegley, 1998). The concentrations of all elements of the Jinju samples plotted on a straight line passing the origin with a slope = 1, which means the chemical compositions of the Jinju meteorite correlate with those of H chondrites. In contrast, some elements in L, LL, and R chondrites plotted off the line. In particular, the Fe concentrations differed significantly among the classes of chondrites. The Fe/Si atomic ratios were 0.81 and 0.83 for Jinju-1 and Jinju-2, respectively. These values agree with 0.80 for H chondrites but differ significantly from the values for other chondrites such as 0.59, 0.53, and 0.68 for L, LL, and R, respectively (Lodders and Fegley, 1998).

These elemental compositions support the H chondrite classification reported for Jinju meteorite (Choi *et al*., 2015).

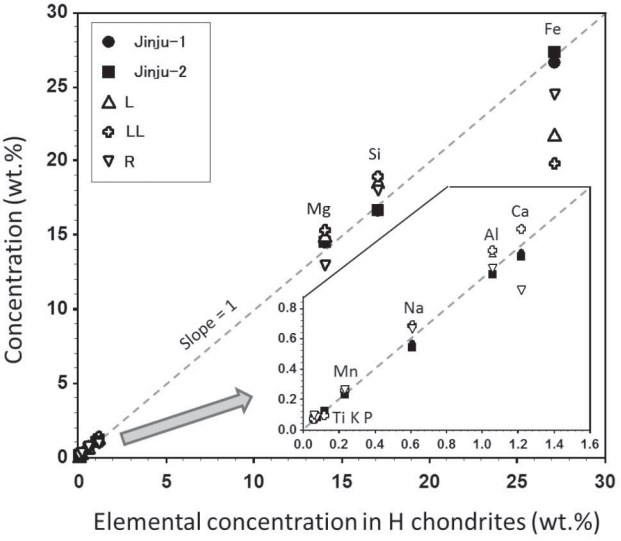

Fig. 1. Chemical compositions of Jinju-1, Jinju-2, L, LL, and R chondrites compared with those of H chondrites. The chemical compositions of Jinju-1 and Jinju-2 are given in Table 1. The data sources for H, L, LL, and R chondrites are from Lodders and Fegley (1998).

Noble gases

The noble gas isotopic compositions and concentrations are presented in Supplementary Tables S1, S2, and S3 in Supplementary Materials. Experimental errors for the isotopic ratios given in the tables were 1σ, whereas the uncertainties in sensitivity and blank correction resulted in an error of 10% for the concentrations.

The rapid recovery is cited as the main reason for the lack of atmospheric noble gas contamination in the meteorite, as indicated by the isotopic ratios and release profiles presented below. A trace amount of contamination from the atmosphere was indicated only for ^{40}Ar/^{36}Ar ratio at the lowest heating temperature of 300°C, which is attributed to the abundance of ^{40}Ar in the terrestrial atmosphere (e.g., Ozima and Podosek, 2002).

Jinju-1 and Jinju-2 showed almost identical noble gas compositions. Moreover, the release profiles for all noble gases from He to Xe were identical among the Jinju-1 and Jinju-2 samples, which suggests homogeneous mineralogical and petrological compositions among the two rocks even at a small scale of less than ~100 mg.

These observations indicate that the two stones recovered separately were derived from a single preatmospheric body of homogeneous composition. The meteorite includes a negligible amount of atmospheric noble gas contamination, as indicated by the Ne and Xe isotopic ratios,

Table 2. Cosmogenic and trapped noble gases in Jinju-1 and Jinju-2

Temp.		$[^3He]_{cosm}$	$[^{21}Ne]_{cosm}$	$[^{38}Ar]_{cosm}$	$[^{20}Ne]_{trap}$	$[^{36}Ar]_{trap}$	$^{40}Ar/^{36}Ar_{trap}$	$^{36}Ar_{trap}/^{132}Xe$	$^{84}Kr/^{132}Xe$	$^{129}Xe/^{132}Xe$
		10^{-9} cc/g								
Jinju-1 130.5 mg										
300		1.85	0.23	0.0017	ND	0.08	2783	96.5	3.08	1.186
	±	0.19	0.02	0.0002		0.01	415	14.1	0.44	0.032
800		30.72	0.99	0.217	ND	4.32	4416	1239.0	35.86	1.074
	±	3.08	0.10	0.026		0.43	681	175.6	5.08	0.023
1100		8.92	2.05	0.261	ND	2.13	4395	360.6	9.65	1.453
	±	0.89	0.22	0.029		0.21	676	51.0	1.36	0.022
1400		6.14	2.08	0.399	0.143	3.96	2925	68.9	1.50	1.239
	±	0.62	0.21	0.040	0.019	0.40	427	9.7	0.21	0.016
1800		0.91	0.90	0.099	0.298	1.67	1008	43.6	0.88	1.363
	±	0.09	0.09	0.010	0.032	0.17	143	6.2	0.13	0.011
Total		48.54	6.44	0.978	0.269	12.17	3448	114.8	2.88	1.290
	±	3.27	0.47	0.205	0.345	0.66	295	9.7	0.24	0.085
Jinju-1 22.1 mg										
1800		48.28	6.62	0.886	0.644	12.02	3760	113.3	2.99	1.237
Total melt	±	4.84	0.66	0.091	0.079	1.20	560	16.1	0.42	0.016
Jinju-2 49.9 mg										
300		1.44	0.20	0.0012	ND	0.22	953	208.8	4.69	1.136
	±	0.14	0.02	0.0003		0.02	136	30.5	0.68	0.080
800		26.36	0.82	0.176	ND	3.78	4453	1505.3	43.20	1.081
	±	2.64	0.08	0.019		0.38	681	212.7	6.10	0.051
1100		10.60	2.53	0.292	ND	2.49	4593	277.8	6.66	1.224
	±	1.06	0.26	0.033		0.25	700	39.4	0.94	0.022
1400		5.57	1.87	0.371	0.213	4.48	2156	55.2	1.14	1.172
	±	0.56	0.19	0.039	0.027	0.45	310	7.8	0.16	0.014
1800		0.85	0.65	0.099	0.250	1.67	800	50.3	0.88	1.254
	±	0.09	0.06	0.010	0.027	0.17	114	7.1	0.13	0.013
Total		44.82	6.07	0.939	0.528	12.63	3123	99.6	2.32	1.201
	±	2.90	0.46	0.206	0.342	0.67	262	8.7	0.20	0.079
Q (Busemann, 2000)								76	0.81	1.042

and no obvious release of Xe at 300°C, as will be subsequently explained in Section "Discussion".

A characteristic feature is the bimodal release of trapped Ar and Kr from the samples; two release peaks at 800°C and 1400°C were present with a dent at 1100°C. In contrast, the trapped Xe showed only one release peak at 1400°C and no peak at 800°C.

The isotopic ratios of He and Ne indicate no obvious solar wind gas in the Jinju meteorite. HL-gas in presolar diamonds can also be ignored for such a high petrologic type of ordinary chondrite owing to its weakness as a carrier in thermal processing (e.g., Huss and Lewis, 1994b).

The following isotopic ratios were used for partitioning noble gas isotopes among different end members (e.g., Eugster, 1988; Eugster *et al.*, 1993): $(^3He/^4He)_{cosm} = 0.2$, $(^{20}Ne/^{22}Ne)_{cosm} = 0.80$, $(^{21}Ne/^{22}Ne)_{cosm} = 0.90$, $(^{38}Ar/^{36}Ar)_{cosm} = 1.55$, $(^{20}Ne/^{22}Ne)_{trap} = 10.67$ (Ne-Q), $(^{21}Ne/^{22}Ne)_{trap} = 0.0294$ (Ne-Q), and $(^{38}Ar/^{36}Ar)_{trap} = 0.188$, in which subscripts "cosm" and "trap" indicate cosmogenic and trapped, respectively, and "Q" indicates a component trapped in the HF/HCl acid residue of primitive chondrites (e.g., Lewis *et al.*, 1975; Busemann *et al.*, 2000; Ott, 2002). The aforementioned isotopic ratios of cosmogenic Ne agree well with those of the 1100°C fraction of the Jinju meteorite. No correction for a cosmogenic component was applied to Kr and Xe. The calculated data are summarized in Table 2.

Cosmogenic and radiogenic He The isotope ratios of $^3He/^4He$ and the ^4He release profiles from stepwise heating are presented in Figs. 2a and 2b, respectively. A prominent release peak of ^4He occurred at a relatively low heating temperature of 800°C, followed by rapid decrease at higher temperatures. The released amounts of ^4He from each heating step varied more than one order of magnitude. This result may be attributed to a lower retention of

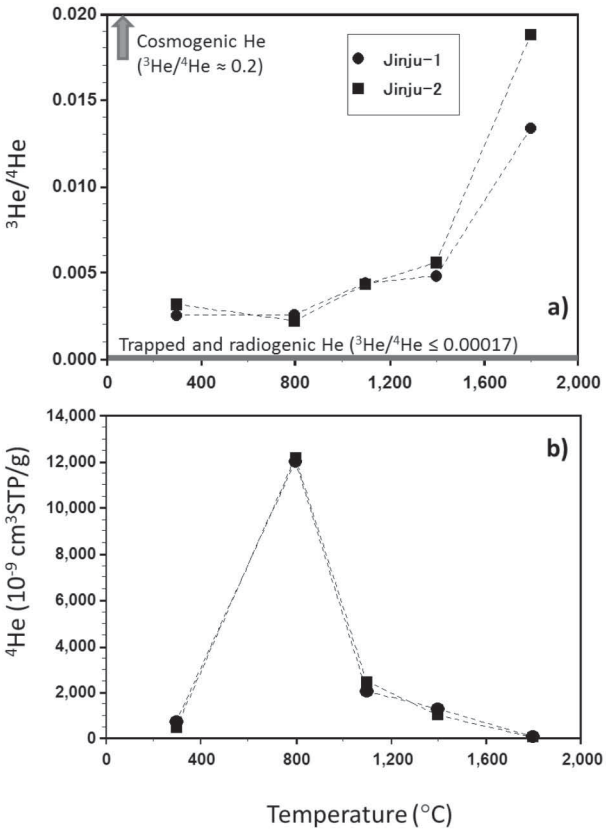

Fig. 2. Plots of a) ^{3}He/^{4}He ratios and b) release profiles of ^{4}He from the stepwise heating experiment performed on Jinju-1 and Jinju-2 samples. Experimental errors for isotope ratios are within the symbols. The ^{3}He/^{4}He ratios for trapped He are 0.00048 for solar wind (Heber et al., 2009), 0.00017 for HL (Huss and Lewis, 1994a), and 0.000123 for Q (Busemann et al., 2000).

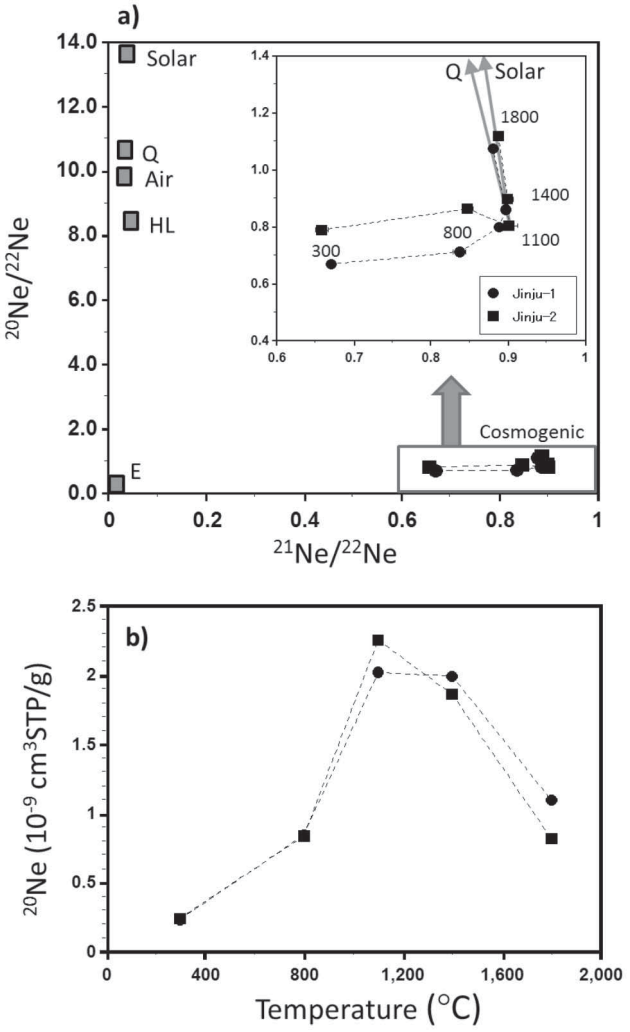

Fig. 3. a) Ne three-isotope plot and b) release profiles of ^{20}Ne. Experimental errors for the isotope ratios are within the symbols. The numerical figures in a) are heating temperatures in °C. Data sources: solar wind (solar), Heber et al. (2009); air, Eberhardt et al. (1965); E, Lewis et al. (1994); HL, Huss and Lewis (1994b); Q, Busemann et al. (2000).

He in the minerals of the meteorite containing U/Th, which has been observed in other meteorites (e.g., Nagao *et al*., 2008; Eugster *et al*., 1993). The ^{3}He/^{4}He ratios were almost constant between 0.0025 and 0.0056 except for higher ratios of 0.013–0.019 for a minor release of ^{4}He at 1800°C. The 0.0025–0.0056 ratios are two orders of magnitude lower than the cosmogenic He (^{3}He/^{4}He ≈ 0.2) and one order of magnitude higher than those of trapped He in carbonaceous chondrites and unequilibrated ordinary chondrites such as ^{3}He/^{4}He = 0.00017 for He-HL in presolar diamonds (Huss and Lewis, 1994a), 0.000123 for He-Q in HF/HCl etching residue (Lewis *et al*., 1975; Busemann *et al*., 2000), and 0.000464 in solar wind (Heber *et al*., 2009).

Because a trapped Ne component is absent from the Jinju meteorite, as shown in Fig. 3a, an absence of trapped He can be reasonably assumed for this meteorite, and the observed He should be a mixture between cosmogenic and radiogenic ^{4}He from the α-decay of U and Th. The low concentrations of cosmogenic ^{3}He, (45–49) × 10^{-9} cm^{3}STP/g, indicate a short cosmic ray exposure age for this meteorite.

Cosmogenic isotopic ratios of Ne The isotopic ratios of Ne and release profiles of ^{20}Ne are shown in Figs. 3a and 3b, respectively. The Ne isotopic ratios of the Jinju meteorite are restricted to a narrow range representing cosmogenic Ne, indicating an almost complete absence of trapped Ne components. Small amounts of ^{20}Ne ≈ 0.23 × 10^{-9} cm^{3}STP/g with a low ^{21}Ne/^{22}Ne (≈0.66) was released at the lowest heating temperature, 300°C. This cosmogenic Ne must have been produced in Na-rich min-

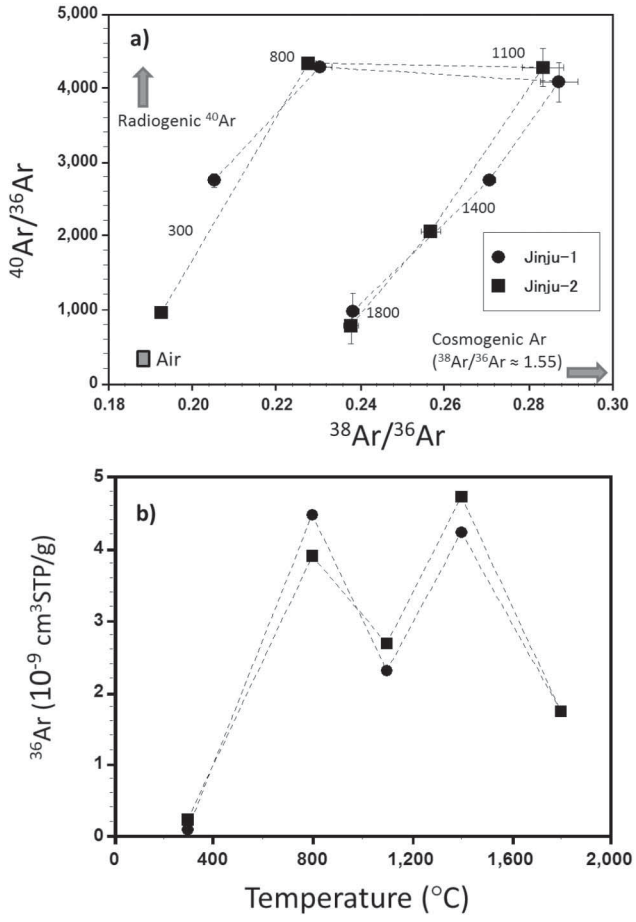

Fig. 4. a) Plot of ^{40}Ar/^{36}Ar versus ^{38}Ar/^{36}Ar and b) release profiles of ^{36}Ar. The numerical figures in a) are the heating temperatures in °C. Data source: air (Nier, 1950).

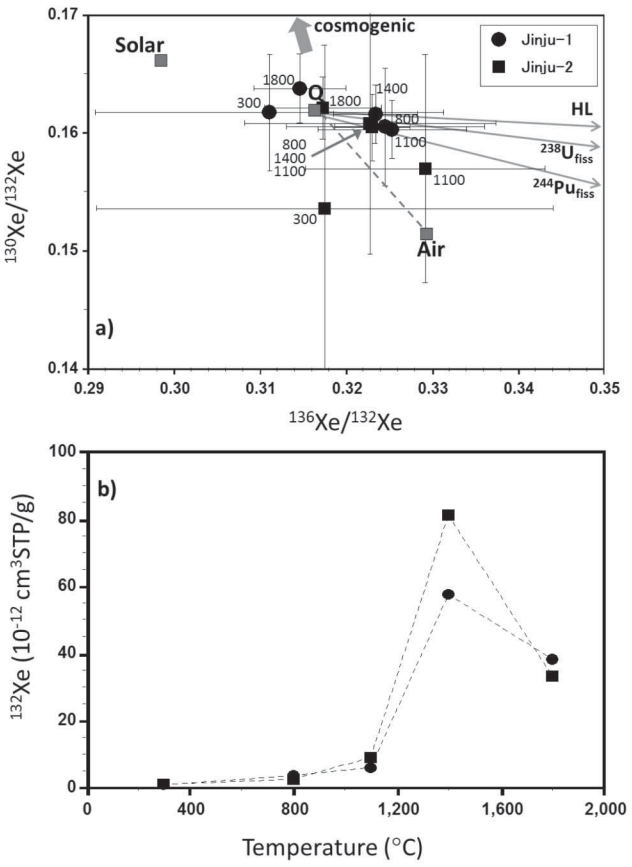

Fig. 5. a) Plot of ^{130}Xe/^{132}Xe versus ^{136}Xe/^{132}Xe and b) release profiles of ^{132}Xe. The numerical figures in a) are the heating temperature in °C. The subscript "fiss" indicates fission. Data sources: Ozima and Podosek (2002), Ott (2002).

erals not resistant to heating, as reported by Smith and Huneke (1975). The enrichment of ^{22}Ne, i.e., low ^{21}Ne/^{22}Ne, in Na-rich minerals, was caused by indirect production of ^{22}Ne through ^{22}Na ($T_{1/2}$ = 2.6 y) from ^{23}Na. At higher temperatures, the Ne isotopic ratios are representative of normal cosmogenic Ne; the ^{21}Ne/^{22}Ne ratios were in the range of 0.85–0.9 for most ordinary chondrites, showing peak releases at 1100°C and 1400°C. This cosmogenic Ne is produced in major minerals such as pyroxene and olivine (e.g., Bogard and Cressy, 1973), which are more resistant to heating than Na-rich minerals.

Slightly higher ^{20}Ne/^{22}Ne ratios, at ~1.1, were observed at 1800°C than those at lower temperatures. These data points as well as those for 1400°C appeared to plot along the mixing lines between Jinju-2 (1100°C) and Ne-Q or Ne-solar wind. This result may indicate the presence of a small concentration of trapped Ne, which is likely Ne-Q because of its high resistance to heating as shown in Xingyang H5 chondrite (Eugster *et al.*, 1993) and HF/HCl residues (Huss *et al.*, 1996).

Isotopic ratios and bimodal release of Ar The Ar isotopic ratios and the release profiles of ^{36}Ar are plotted in Figs. 4a and 4b, respectively. The concentrations of trapped ^{36}Ar, $(1.2–1.3) \times 10^{-8}$ cm^{3}STP/g (Table 2), are in the range typical for chondrites of petrologic type 5–6 (Marti, 1967), which is consistent with the classification of H5 for the Jinju meteorite (Choi *et al.*, 2015). The bimodal release of ^{36}Ar at temperatures of 800°C and 1400°C with a dent at 1100°C was observed. Trace contamination from atmospheric Ar is indicated at the lowest heating temperature of Jinju-2, 300°C. At that temperature, the ratios of both ^{38}Ar/^{36}Ar = 0.193 and ^{40}Ar/^{36}Ar = 949 were closer to the composition of air at ^{38}Ar/^{36}Ar = 0.188 and ^{40}Ar/^{36}Ar = 296 (Nier, 1950) than other data points plotted in Fig. 4a. Moreover, only small amounts of Ar were released from Jinju-1 and Jinju-2 at that temperature, i.e., 0.67–1.6% and 0.53–0.56% of the total ^{36}Ar and ^{40}Ar, respectively. Jinju-1 appears to be

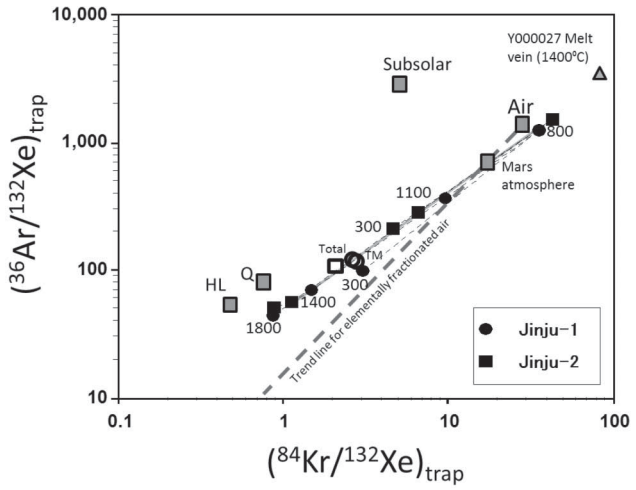

Fig. 6. Plot of $^{36}Ar/^{132}Xe$ versus $^{84}Kr/^{132}Xe$. The numerical figures and "Total" are heating temperatures in °C and the sum of data obtained by stepwise heating, respectively. "TM" is the total melt of Jinju-1. The solid straight line between 800°C and 1400°C data points is the mixing line. Data sources: ($^{36}Ar/^{132}Xe$, $^{84}Kr/^{132}Xe$) = Q (76, 0.81), HL (50, 0.48), and subsolar (2660, 5.86): Ott (2002); air (1340, 27.7) and Mars atmosphere (595, 20.7): Ozima and Podosek (2002); trend line for elementally fractionated air: Nagao (1994); Y000027 melt vein (1400°C): Nagao et al. (2008).

less contaminated by atmospheric Ar than Jinju-2, which might reflect the earlier recovery of Jinju-1. The $^{40}Ar/^{36}Ar$ ratios were as high as 4280–4320 and 4070–4270 at temperatures of 800°C and 1100°C, respectively. The higher $^{38}Ar/^{36}Ar$ ratios at the latter temperature indicate a larger contribution of cosmogenic Ar to trapped Ar at 1100°C. At the second release peak of ^{36}Ar, 1400°C, the $^{40}Ar/^{36}Ar$ ratios decreased to about half of the highest ratios. These data indicate that radiogenic ^{40}Ar produced by the decay of ^{40}K is released at relatively low heating temperatures likely from K-rich minerals such as plagioclase, which are not strongly resistant to heating. Conversely, the Ar gas released at the second peak is likely from thermally resistive and K-poor minerals with relatively higher concentrations of primordial Ar. One of the candidates for the carriers is phase-Q, which is known to have very high concentrations of primordial Ar, Kr, and Xe (e.g., Lewis *et al*., 1975; Busemann *et al*., 2000) and is also resistive to heating; Q gases are usually extracted from primitive chondrites at temperatures higher than 1000°C (e.g., Huss *et al*., 1996).

Q-like isotope composition and different release profiles of Kr and Xe The concentrations of trapped ^{132}Xe at (1.1–1.3) $\times 10^{-10}$ cm^3STP/g, as shown in Table S1, are at the lower end of chondrites of petrologic type 6 ($^{132}Xe < 1.4 \times 10^{-10}$ cm^3STP/g; Marti, 1967). This may suggest a higher petrologic type than type 5 for the Jinju meteorite. In contrast, the ^{84}Kr concentrations, at (3.0–3.6) $\times 10^{-10}$ cm^3STP/g, are in the range for type 4 (figure 1 in Marti, 1967). The larger abundance of trapped ^{84}Kr than that expected from the petrologic type 5 is attributed to the Kr (and Ar) trapped in minerals/phases less retentive to heating than phase-Q, as is discussed subsequently.

A bimodal release of ^{84}Kr was observed with peaks at 800°C and 1400°C (Table S2), which is similar to that of ^{36}Ar (Fig. 4b). The isotopic ratios of Kr are within the range for Kr-Q or atmospheric Kr within error limits. The release profiles of ^{132}Xe (Fig. 5b), however, show a single release peak at a high temperature of 1400°C followed by a substantial release at the melting of the samples at 1800°C. Only a small amount of Xe was released at low temperatures of 300°C, 800°C, and 1100°C, indicating small amounts of air contamination that should have been released at ≤300°C. Another important point is the absence of the Xe component released at these heating temperatures. Xe is expected to have been released at 800°C with trapped Ar and Kr (Fig. 4b) because the trapped component of heavy Ar, Kr, and Xe is mostly the Q component, as indicated in the isotopic ratios (Fig. 5a; Tables S2 and S3) and elemental compositions (Fig. 6). A plot of $^{130}Xe/^{132}Xe$ versus $^{136}Xe/^{132}Xe$ ratios (Fig. 5a) shows that the Xe is mostly Xe-Q, although atmospheric contamination is indistinguishable within the error limits. The contribution of cosmogenic Xe to ^{130}Xe and ^{132}Xe was also negligible, as indicated in Fig. 5a. The large error bars for data points at low temperatures are attributed to small amounts of Xe released from the samples, as shown in Fig. 5b. Xe-HL, formerly CCF-Xe or Xe-X (e.g., Manuel *et al*., 1972a), is released in a similar temperature range from 800°C to 1000°C when bulk carbonaceous chondrites are heated stepwise (e.g., Reynolds and Turner, 1964; Manuel *et al*., 1972b). Xe-HL is, however, unlikely because presolar diamonds, carriers of the HL component, are not resistant to metamorphic heating (Huss and Lewis, 1995). The Jinju meteorite (H5) is highly metamorphosed and was affected by heavy shock events (Choi *et al*., 2015). ^{244}Pu ($T_{1/2} = 8.0 \times 10^7$ y) is difficult to ignore as a candidate of fissiogenic Xe, although it is not common in ordinary chondrites. Trace amounts of ^{129}Xe from the extinct ^{129}I ($T_{1/2} = 1.57 \times 10^7$ y) are present in this meteorite because the $^{129}Xe/^{132}Xe$ ratios, at 1.007–1.45, are slightly higher than the ratios of Xe-Q, at 1.042 (Busemann *et al*., 2000; Ott, 2002). The $^{129}Xe/^{132}Xe$ data do not exclude the possible presence of Xe from ^{244}Pu fission owing to the longer half-life of ^{244}Pu than that of ^{129}I.

Overabundances of trapped Ar and Kr in low-temperature fraction The $^{36}Ar/^{132}Xe$ versus $^{84}Kr/^{132}Xe$ ratios of trapped gases are shown in Fig. 6 and in Table 2. All of the data points appear to plot on a single straight line in

Table 3. Cosmic-ray exposure ages, and U,Th-He and K-Ar gas retention ages of Jinju-1 and Jinju-2

Sample	$^{3}He/^{21}Ne$	$^{22}Ne/^{21}Ne$	P_3	P_{21}	P_{38}	T_3	T_{21}	T_{38}	average	^{4}He-rad	^{40}Ar-rad	U,Th-He (T_4)	K-Ar (T_{40})	T_3/T_{21}	T_4/T_{40}
			10^{-8} cm^{3}STP/g/My			My				10^{-5} cm^{3}STP/g		Gy			
Jinju-1 (Step heat)	7.54	1.15	1.57	0.266	0.0484	3.10	2.25	2.02	2.46	1.59 ± 0.12	4.20 ± 0.28	3.98 ± 0.17	3.90 ± 0.19	1.38	1.02
Jinju-1 (Total melt)	7.29	1.16	1.56	0.252	0.0473	3.10	2.44	1.87	2.47	1.15 ± 0.12	4.52 ± 0.50	3.24 ± 0.22	4.01 ± 0.24	1.27	0.81
Jinju-2 (Step heat)	7.39	1.13	1.57	0.280	0.0493	2.85	2.02	1.90	2.26	1.59 ± 0.13	3.95 ± 0.26	3.99 ± 0.17	3.80 ± 0.19	1.42	1.05

the log-log plot. This line differs from a trend line for the elementary fractionated terrestrial atmosphere observed for rocks derived from Earth's mantle as shown in Fig. 6 (Nagao, 1994), on which Mars atmosphere and Martian meteorites (e.g., Ott, 1988; Nagao *et al*., 2008), well-degassed meteorites such as howardite-eucrite-diogenites (HEDs), Brachina, and silicates in a pallasite are also plotted (Nagao, 1994).

The $^{36}Ar/^{132}Xe$ and $^{84}Kr/^{132}Xe$ ratios obtained by the total melting of Jinju-1 and the sum of all temperature fractions for Jinju-1 and Jinju-2 are 100–115 and 2.3–3.0, respectively (Table 2). These ratios are clearly higher than those of Q gas, which may indicate an overabundance of trapped Ar and Kr to the Q component. Gases released at 1400°C, which is the second peak for ^{36}Ar shown in Fig. 4b and for ^{84}Kr, and 1800°C have Q-like elemental ratios (Table 2). However, the slightly lower $^{36}Ar/^{132}Xe$ ratios at 1800°C, at 44 and 50 for Jinju-1 and Jinju-2, respectively, than those of the 1400°C fraction are the likely result of elemental fractionation that occurred during the stepwise heating. The Q-like elemental composition is compatible with the Q-like isotopic ratios of Xe (Fig. 5a). On the contrary, the first release peaks of ^{36}Ar (Fig. 4b) and ^{84}Kr and a small release of ^{132}Xe at 800°C (Fig. 5b) showed unusually high $^{36}Ar/^{132}Xe$ and $^{84}Kr/^{132}Xe$ ratios of (1240, 36) and (1510, 43) for Jinju-1 and Jinju-2, respectively. Data points at other temperatures plotted on a straight line, which appears to be a mixing line between the aforementioned two temperature fractions, 800°C and 1400°C, even though a log-log plot is indicated in the figure.

Higher $^{36}Ar/^{132}Xe$ at 3120 and $^{84}Kr/^{132}Xe$ at 76 were observed for the 1400°C fraction of a shock-produced melt vein from Martian meteorite Y-000027 shergottite (Nagao *et al*., 2008). The data point appeared to plot around an extension of the mixing line. In the case of the melt vein from Y-000027, bimodal releases of ^{36}Ar and ^{84}Kr at 800°C and 1400°C were observed, although ^{132}Xe was released at higher temperatures of 1600°C and 1800°C with a single release peak. The Jinju meteorite is also heavily shocked at S3 or higher (Choi *et al*., 2015); therefore, elemental fractionation induced by the shock may have produced high $^{36}Ar/^{132}Xe$ and $^{84}Kr/^{132}Xe$.

DISCUSSION

Cosmic-ray exposure age

The total concentrations of cosmogenic ^{3}He, ^{21}Ne, and ^{38}Ar shown in Table 2 were used to calculate the cosmic ray exposure ages of this meteorite. The production rates of ^{3}He, ^{21}Ne, and ^{38}Ar were calculated following the method proposed by Herzog (2005). The $^{22}Ne/^{21}Ne$ ratios in Table 3 were used to correct shielding depth against cosmic-ray irradiation. Because the production rates are

given for L chondrites in Herzog (2005), the concentrations of elements in Table 1 were used to calculate the correction factors for the target element compositions from L chondrites to the Jinju H chondrite. The $^{3}He/^{21}Ne$ and $^{22}Ne/^{21}Ne$ for cosmogenic He and Ne in Table 3, 7.29–7.54 and 1.13–1.16, respectively, plotted slightly above the correlation line for chondrites in the Bern plot of $^{3}He/^{21}Ne$ versus $^{22}Ne/^{21}Ne$ (e.g., Eugster, 1988). This result indicates that the concentration of cosmogenic ^{3}He in the Jinju meteorite is higher than that of most ordinary chondrites. The cosmic ray exposure ages calculated by using the concentrations of cosmogenic ^{3}He, ^{21}Ne, and ^{38}Ar for three samples are T_3 = 2.85–3.10 My, T_{21} = 2.02–2.44 My, and T_{38} = 1.90–2.02 My, respectively. The ages based on each isotope are in fairly good agreement, although the T_3 exposure age is longer than that for T_{21} and T_{38}; the reason for this discrepancy is not clear at present. However, this result indicates complete retention of He in the meteorite during the period of cosmic ray exposure. The average value for all ages is 2.4 ± 0.5 My. The cosmic ray exposure age obtained for the Jinju meteorite is significantly shorter than the enhanced peak at 6–8 My of H5 chondrites in the histogram (e.g., Eugster *et al*., 1993; Herzog, 2005), which shows that the ejection of the Jinju meteorite from its parent asteroid was independent of the 6–8 My event. The concentrations of cosmogenic He, Ne, and Ar and the exposure ages noted above clearly indicate that the pre-atmospheric body of the Jinju meteorite had not been sufficiently heated to lose light noble gases in space for 2.4 My after ejection from its parent asteroid.

(U,Th)-He and K-Ar gas retention ages

The concentrations of radiogenic ^{4}He and ^{40}Ar are given in Table 3. Cosmogenic ^{4}He was subtracted from the measured ^{4}He by using $(^{3}He/^{4}He)_{cosm}$ = 0.2, and the measured ^{3}He was assumed to be totally cosmogenic. On the basis of the previous discussion, the measured ^{40}Ar was assumed to be radiogenic from ^{40}K, neglecting air contamination; the contribution of ^{4}He derived from ^{244}Pu was also ignored. The (U,Th)-He and K-Ar ages were calculated by using the average concentrations of Th, at 42 ppb; U, at 12 ppb (Wasson and Kallemeyn, 1988); and K, at 782 ppm (Kallemeyn *et al*., 1989) for H chondrites. The calculated (U,Th)-He and K-Ar ages are 3.2–4.0 Gy and 3.8–4.0 Gy, respectively. These nearly identical (U,Th)-He and K-Ar ages indicate no thermal disturbance in the Jinju parent asteroid after the heating event, which almost completely reset these chronological systems at ~4.0 Gy. Otherwise, the (U,Th)-He age would have been shorter than the K-Ar age owing to the preferential loss of He during incomplete heating, as shown in figure 13 of Eugster *et al*. (1993).

A comparison of the cosmic ray exposure ages based on ^{3}He and ^{21}Ne and the (U,Th)-He and K-Ar ages in a T_3/T_{21} versus T_4/T_{40} diagram, as discussed in Eugster *et al*. (1993), indicates that no thermal event occurred to cause the escape of He from the parent body of the Jinju meteorite or from the Jinju meteoroid itself throughout ~4.0 Gy.

Bimodal release profiles of trapped Ar and Kr

The Xe isotopic composition shown in Fig. 5a indicates that trapped heavy noble gases, Ar, Kr, and Xe, are comparable with the Q component trapped in the Q phase. Xe was retained at a temperature lower than 1100°C in the stepwise heating experiment and began to be released at higher temperatures with a release peak at 1400°C (Fig. 5b). The release profile of Xe is typical for the Q component in most carbonaceous chondrites (e.g., Manuel *et al*., 1972b), ordinary chondrites such as the Otis L6 (Eugster, 1988) and Xingyang H5 chondrites (Eugster *et al*., 1993), and HF/HCl residues (Huss *et al*., 1996). In contrast to Xe, both ^{36}Ar (Fig. 4b; Table 2) and ^{84}Kr (Tables S1 and S2) exhibited bimodal release with peaks at 800°C and 1400°C. Moreover, the $^{84}Kr/^{132}Xe$ ratios of total gases were 2.88 and 2.99 for Jinju-1 and 2.32 for Jinju-2 (Table 2), which are significantly higher than the ratio of 0.56–1.00 (average 0.81) of the Q component (Busemann *et al*., 2000). The $^{36}Ar_{trap}/^{132}Xe$ ratios of 115 and 113 for Jinju-1 and 100 for Jinju-2 shown in Table 2 are also higher than the 53–105 Q value (average 76; Busemann *et al*., 2000).

The high $^{36}Ar_{trap}/^{132}Xe$ and $^{84}Kr/^{132}Xe$ ratios for the Jinju meteorite are attributed mainly to the release of trapped ^{36}Ar and ^{84}Kr at 800°C and 1100°C, where very high $^{36}Ar_{trap}/^{132}Xe$ and $^{84}Kr/^{132}Xe$ ratios up to 1500 and 43.2 (Table 2), respectively, were observed. However, $^{36}Ar_{trap}/^{132}Xe$ and $^{84}Kr/^{132}Xe$ ratios of 62 and 1.25 for Jinju-1 and 56 and 1.07 for Jinju-2 were obtained for total 1400°C and 1800°C fractions, where almost all of the Xe was released from the samples. These ratios are much closer to those of the Q component, unlike the ratios for the 800°C and 1100°C fractions.

In simplified expression, the heavy noble gas compositions in the Jinju meteorite can be explained by an overprint of Q-like Ar and Kr on Q gases originally incorporated into the Jinju parent body.

This observation may indicate that the Q phase in the Jinju meteorite was not severely damaged. Rather, the Ar and Kr overprinting might have been supplied from a different source and was trapped later in some minerals and phases, which released the trapped gases at low temperatures of ≤800°C. After the H chondritic asteroid metamorphosed the material to petrologic type 5–6, the Jinju meteoroid incurred the effects of heavy shock by impact at stage S3 or higher (Choi *et al*., 2015). If the impact occurred close to the area in which the Jinju meteoroid

was located, the propagated shock energy increased the temperature of the Jinju meteoroid for a short period, which was followed by rapid cooling. The impact likely reset the (U,Th)-He and K-Ar chronometers at about 4.0 Gy. The heating condition needed to be such that no Q gas was lost from the Jinju meteorite while still being above the temperature to reset the chronometers. Considering that the temperatures were sufficient to reset the K-Ar system and the Q phase was maintained, the peak temperature was *ca*. 800–1000°C. If elementally fractionated Q gas resulting from selective release of gases lighter than Xe was transported from a shock-heated area to the Jinju meteoroid, Ar and Kr might have been trapped in the solidifying minerals or phases less resistant to heating than those of the Q phase. The mechanism for releasing gas enriched in Ar and Kr from the Q phase while leaving Xe during the shock heating, however, is difficult to clarify at present. Stepwise heating experiments conducted on the Xingyang H5 chondrite (Eugster *et al*., 1993) and HF/HCl residues from unequilibrated chondrites (Huss *et al*., 1996) did not show significant elemental fractionation. However, Huss *et al*. (1996) compared Q gas in several different petrologic types of enstatite chondrites and suggested that "subsolar" gases could be released from enstatite and become acquired by a carbonaceous P1 (Q) carrier during a brief melting episode. Moreover, the significant elemental fractionation observed in the shock-produced melt vein from the Y-000027 shergottite (Nagao *et al*., 2008) shown in Fig. 6 indicates that a dynamical process such as shock heating plays an important role in the elemental fractionation. These results suggest that the shock-produced melt can acquire elementally fractionated Q gas released from the Q phase and transfer the gas elsewhere. Vaporized gases produced by the shock heating may have expanded to adjacent regions, resulting in porous structures and vapor-growth crystals such as those found in the Jinju meteorite (Choi *et al*., 2015). The trapping sites of the low-temperature-released Ar and Kr in the Jinju meteorite are still unknown. *In vacuo* crushing experiments and mineral separation of the Jinju meteorite would be effective for clarifying the trapping sites of Ar and Kr released at low-temperature heating <800°C.

Acknowledgments—The authors greatly appreciate the owners the four stones of the Jinju meteorite, Won-Ki Kang, Sand-Duk Park, Ju-Young Lee, and Man-Shik Kim, for providing us with specimens for scientific investigation. The authors are also indebted to Sang Bum Park and In Sung Yu for their work on sample preparations in the cleaning, cutting, and creation of polished thin sections of the meteorite samples. In addition, the authors are grateful to M. M. M. Meier and an anonymous reviewer for their valuable input that improved the quality of the manuscript. K.N. acknowledges the Ministry of Science, ICT and Planning (MSIP) of Korea for supporting the research work on the Jinju meteorite. This study was supported by the Korea Ministry of Ocean and Fisheries R&D grant No. PM15030.

References

Bogard, D. D. and Cressy, P. J., Jr. (1973) Spallation production of ^{3}He, ^{21}Ne, and ^{38}Ar from target elements in the Bruderheim chondrite. *Geochim. Cosmochim. Acta* **37**, 527–546.

Busemann, H., Baur, H. and Wieler, R. (2000) Primordial noble gases in "phase Q" in carbonaceous and ordinary chondrites studied by closed-system stepped etching. *Meteor. Planet. Sci*. **35**, 949–973.

Choi, B.-G., Kim, H., Kim, H., Lee, J. I., Kim, T. H., Ahn, I., Yi, K. and Hong, T. E. (2015) Jinju H5 chondrite: a new fall in Korea having numerous vugs filled with vapor-phase crystallized minerals. *78th Annual Meeting of the Meteoritical Society*, 5091.pdf.

Eberhardt, P., Eugster, O. and Marti, K. (1965) A redetermination of the isotopic composition of atmospheric neon. *Zeitschrift für Naturforschung* **20a**, 623–624.

Eugster, O. (1988) Cosmic-ray production rates for ^{3}He, ^{21}Ne, ^{38}Ar, ^{83}Kr, and ^{126}Xe in chondrites based on ^{81}Kr-Kr exposure ages. *Geochim. Cosmochim. Acta* **52**, 1649–1662.

Eugster, O., Michel, T., Niedermann, S., Wang, D. and Yi, W. (1993) The record of cosmogenic, radiogenic, fissiogenic, and trapped noble gases in recently recovered Chinese and other chondrites. *Geochim. Cosmochim. Acta* **57**, 1115–1142.

Fitton, J. G. and Godard, M. (2004) Origin and evolution of magmas on the Ontong Java Plateau. *Geol. Soc. London Spec. Publ*. **229**, 151–178.

Fitton, J. G., Saunders, A. D., Larsen, L. M., Hardarson, B. S. and Norry, M. J. (1998) Volcanic rocks from the southeast Greenland margin at 63°N: Composition, petrogenesis and mantle sources. *Proceedings of the Ocean Drilling Program. Scientific Results* **152**, 331–350.

Heber, V. S., Wieler, R., Baur, H., Olinger, C., Friedmann, T. A. and Burnett, D. S. (2009) Noble gas composition of the solar wind as collected by the Genesis mission. *Geochim. Cosmochim. Acta* **73**, 7414–7432.

Herzog, G. F. (2005) Cosmic-ray exposure ages of meteorites. *Meteorites, Comets, and Planets* (Davis, A. M., ed.), 347–380, Treatise on Geochemistry Volume 1, Elsevier.

Huss, G. R. and Lewis, R. S. (1994a) Noble gases in presolar diamonds I: Three distinct components and their implications for diamond origins. *Meteoritics* **29**, 791–810.

Huss, G. R. and Lewis, R. S. (1994b) Noble gases in presolar diamonds II: Component abundances reflect thermal processing. *Meteoritics* **29**, 811–829.

Huss, G. R. and Lewis, R. S. (1995) Presolar diamond, SiC, and graphite in primitive chondrites: Abundances as a function of meteorite class and petrologic type. *Geochim. Cosmochim. Acta* **59**, 115–160.

Huss, G. R., Lewis, R. S. and Hemkin, S. (1996) The 'normal planetary' noble gas component in primitive chondrites: Compositions, carrier, and metamorphic history. *Geochim. Cosmochim. Acta* **60**, 3311–3340.

Kallemeyn, G. W., Rubin, A. E., Wang, D. and Wasson, J. T. (1989) Ordinary chondrites: Bulk compositions, classification, lithophile-element fractionations, and composition-petrographic type relationships. *Geochim. Cosmochim. Acta* **53**, 2747–2767.

Lewis, R. S., Srinivasan, B. and Anders, E. (1975) Host phase of strange xenon component in Allende. *Science* **190**, 1251–1262.

Lewis, R. S., Amari, S. and Anders, E. (1994) Interstellar grains in meteorites: II. SiC and its noble gases. *Geochim. Cosmochim. Acta* **58**, 471–494.

Lodders, K. and Fegley, B., Jr. (1998) *The Planetary Scientist's Companion*. Oxford University Press, 371 pp.

Manuel, O. K., Hennecke, E. W. and Sabu, D. D. (1972a) Xe in carbonaceous chondrites. *Nat. Phys. Sci*. **240**, 99–101.

Manuel, O. K., Wright, R. J., Miller, D. K. and Kuroda, P. K. (1972b) Isotopic compositions of rare gases in the carbonaceous chondrites Mokoia and Allende. *Geochim. Cosmochim. Acta* **36**, 961–983.

Marti, K. (1967) Trapped xenon and the classification of chondrites. *Earth Planet. Sci. Lett*. **2**, 193–196.

Nagao, K. (1994) Noble gases in hosts and inclusions from Yamato-75097 (L6), -793241 (L6) and -794046 (H5). *Proceedings of the NIPR Symposium on Antarctic Meteorites* **7**, 197–216.

Nagao, K., Park, J. and Choi, H. G. (2008) Noble gases of the Yamato 000027 and Yamato 000097 lherzolitic shergottites from Mars. *Polar Sci*. **2**, 195–214.

Nagao, K., Kusakabe, M., Yoshida, Y. and Tanyileke, G. (2010) Noble gases in Lakes Nyos and Monoun, Cameroon. *Geochem. J*. **44**, 519–543.

Nagao, K., Okazaki, R., Nakamura, T., Miura, Y. N., Osawa, T., Bajo, K., Matsuda, S., Ebihara, M., Ireland, T. R., Kitajima, F., Naraoka, H., Noguchi, T., Tsuchiyama, A., Yurimoto, H., Zolensky, M. E., Uesugi, M., Shirai, K., Abe, M., Yada, T., Ishibashi, Y., Fujimura, A., Mukai, T., Ueno, M., Okada, T., Yoshikawa, M. and Kawaguchi, J. (2011) Irradiation history of Itokawa regolith material deduced from noble gases in the Hayabusa samples. *Science* **333**, 1128–1131.

Nagao, K., Haba, M. K., Lee, J. I., Kim, T. and Lee, M. J. (2015) Noble gases of the Jinju (H5) meteorite fell on March 9, 2014, in Korea. *78th Annual Meeting of the Meteoritical Society, Berkeley, California*, 5027.pdf.

Nier, A. O. (1950) A redetermination of the relative abundances of the isotopes of carbon, nitrogen, oxygen, argon, and potassium. *Phys. Rev*. **77**, 789–793.

Olsen, E. (1981) Vugs in ordinary chondrites. *Meteoritics* **16**, 45–59.

Ott, U. (1988) Noble gases in SNC meteorites: Shergotty, Nakhla, Chassigny. *Geochim. Cosmochim. Acta* **52**, 1937–1948.

Ott, U. (2002) Noble gases in meteorites—Trapped components. *Noble Gases—In Geochemistry and Cosmochemistry* (Porcelli, D., Ballentine, C. J. and Wieler, R., eds.), *Reviews in Mineralogy and Geochemistry* **47**, 71–100.

Ozima, M. and Podosek, F. A. (2002) *Noble Gas Geochemistry*. 2nd ed., Cambridge University Press, 286 pp.

Reynolds, J. H. and Turner, G. (1964) Rare gases in the chondrite Renazzo. *J. Geophys. Res*. **69**, 3263–3281.

Smith, S. P. and Huneke, J. C. (1975) Cosmogenic neon produced from sodium in meteoritic minerals. *Earth Planet. Sci. Lett*. **27**, 191–199.

Wasson, J. T. and Kallemeyn, G. W. (1988) Compositions of chondrites. *Phil. Trans. Roy. Soc. London* **A325**, 535–544, doi:10.1098/rsta.1988.0066.

Wlotzka, F. and Otto, J. (2001) Euhedral crystals in interstitial pores of the Baszkówka and Mt. Tazerzait L5 chondrites. *Geol. Quart*. **45**, 257–262.

Xie, X. and Chen, M. (1997) Shock-produced vapor-grown crystals in the Yanzhuang meteorite. *Science in China (Series D)* **40**, 113–119.

Supplementary Materials

URL (http://www.terrapub.co.jp/journals/GJ/archives/data/50/MS418.pdf)
Tables S1 to S3